Numerical Study of Lissajous Acceleration for Electrodeless Plasma Thruster

IEPC-2013-210

Presented at the 33rd International Electric Propulsion Conference,
The George Washington University, Washington, D.C., USA
October 6–10, 2013

Ryosuke Nomura*, Naofumi Ohnishi†
Tohoku University, Sendai, Miyagi, 980-8579, Japan

and

Takahiro Nakamura‡, Hiroyuki Nishida§
Tokyo University of Agriculture and Technology, Koganei, Tokyo, 184-8588, Japan

Two-dimensional simulations were conducted by a code based on Particle-In-Cell (PIC) method. for investigating Lissajous acceleration and optimal condition in acceleration area of electrodeless plasma thruster with rotating electric field. Resulting from the simulations without radial magnetic field, the rotating electric field hardly penetrates into moderately dense plasma of 10^{11} cm^{-3} which is considered to be transparent in ideally rigid-rotating plasma, and azimuthal current is reduced. So, we should apply high magnetic field and/or high-frequency electric field to achieve the expected electron acceleration. When the electric field penetrates in a level of 0.6 with respect to the ideal strength, we can obtain the stable azimuthal current. The simulations with the radial magnetic field show that the thrust is proportional to the azimuthal current and the radial magnetic field. However, to eliminate loss of plasma momenta, the radial magnetic field should be lower than 3% of the axial magnetic field.

Nomenclature

m	= particle mass
t	= time
$\boldsymbol{v}$	= particle velocity
q	= particle charge
$\boldsymbol{E}$	= electric field
$\boldsymbol{B}$	= magnetic field
ϵ	= permittivity
ϕ	= electric potential
ρ	= net charge density
L_0	= distance between antennae
L	= plasma region length
V_0	= AC amplitude
f, ω	= AC frequency and angular frequency
n_{p0}	= initial plasma density

*Graduate Student, Department of Aerospace Engineering, nomura@rhd.mech.tohoku.ac.jp
†Associate Professor, Department of Aerospace Engineering
‡Graduate Student, Department of Mechanical Systems Engineering
§Associate Professor, Department of Mechanical Systems Engineering

B_{r0} = radial magnetic field
r = radial distance
J_θ = azimuthal current
R_D = electron drift radius
e = electron charge
m_e = electron mass
ω_{ce} = cyclotron frequency
ω_{pe} = plasma frequency
E_{pg0} = theoretical electric field strength
ς = dimensionless parameter of theoretical electric field strength
F = thrust after 5 AC cycles
i = index of super-particle
n = number density of super-particle
v_z = axial velocity of super-particle

I. Introduction

Plasma thrusters are suitable for long-term space missions such as a sample return mission. An ion thruster called μ10 led the Hayabusa space explorer successfully to accomplish a sample return mission in which the explorer picked surface materials of the asteroid Itokawa.[1] However, sputter erosion of the electrode grid is the critical limitation of life-time in the conventional plasma thrusters.[2] For a longer-term and deeper-space mission, we have to solve the life-time problem due to the electrode erosion. In order to avoid such a problem, several electrodeless plasma thrusters have been proposed by utilizing a helicon plasma source, so far.[3,4]

A configuration of acceleration area of the electrodeless plasma thruster with rotating electric field is shown in Fig. 1. The acceleration area is set on a downstream side of the helicon plasma source along the axial direction of the figure, and two pairs of deflection plate antennae cover it to induce the rotating electric field. Static diverging magnetic field is externally provided in the acceleration area. Plasma motion in a cross section of the area is azimuthal drift due to the rotating electric field and axial magnetic field B_z, and then azimuthal current J_θ is induced. Axial Lorentz force produced by J_θ and radial magnetic field B_r accelerates the plasma to the axial direction. This acceleration is called as Lissajous acceleration. In past studies, the Lissajous acceleration has been theoretically and experimentally investigated toward a proof of principle.[5,6] However, the Lissajous acceleration has interactions between the plasma and the electromagnetic field, and the plasma motion is determined by complicated mechanism originating from many parameters. So, numerical simulations are helpful for understanding the plasma motion in the acceleration area.

Two-dimensional simulations of the Lissajous acceleration have been conducted by a code based on Particle-In-Cell (PIC) method in a cross section of the acceleration area. In the past study, we only investigated the optimal condition of J_θ when plasma number density is relatively low and electric field penetration is ideally.[7] So, we examine dependence of J_θ on the electric field penetration and estimate thrust generation with radial magnetic field in the present paper.

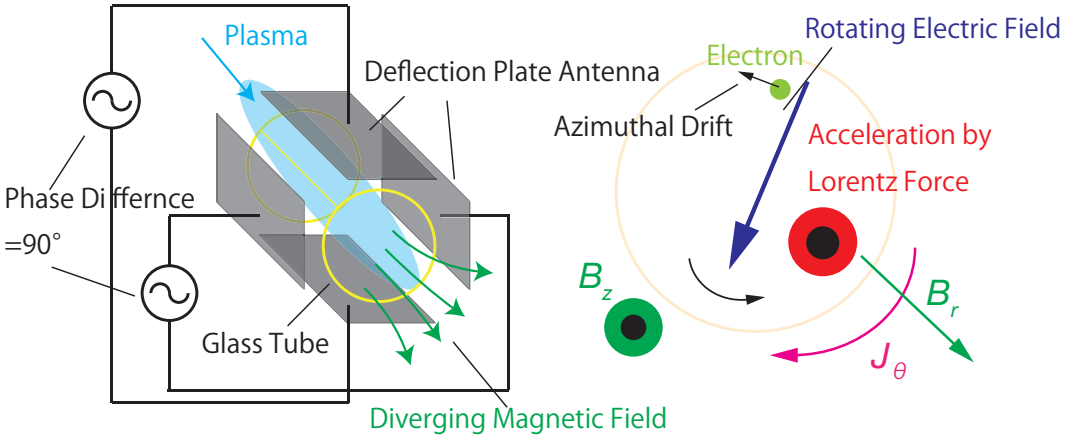

Figure 1. Schematic view of the electrodeless plasma thruster with rotating electric field.

II. Numerical Method

The PIC method takes into account interactions between the charged particles and the electromagnetic field and expresses collisionless plasma by solving the equation of motion for the charged particles.[8] Basic equations for the particle motion and the electric field are given by

$$m\frac{d\boldsymbol{v}}{dt} = q(\boldsymbol{E} + \boldsymbol{v}\times\boldsymbol{B}), \tag{1}$$

$$\nabla\cdot(\varepsilon\nabla\phi) = -\rho, \tag{2}$$

$$\boldsymbol{E} = -\nabla\phi. \tag{3}$$

Neglecting the induction field, we can obtain the electric field by solving the Poisson equation (2) instead of the Maxwell equation. The charge density ρ is estimated by weighted counting with the particle position and the particle charge, so that the system of equations is closed.

Since realistic plasma consists of enormous particles, we cannot calculate the motion of all the particles because of limitations of computational resources. In the PIC method, a concept of super-particle is introduced, which acts as a clump of particles and has fictitious large mass and charge. We give a finite size to the super-particles and distribute their charge to each grid point with a weighting method. Electric interactions among the super-particles are estimated using the distributed charges at the grid points rather than N-body Coulomb forces.

III. Simulation Conditions

In this work, simulation domain is a cross section of the acceleration area as shown in Fig. 2. This domain covers a 2.4-cm × 2.4-cm square with computational cells assuring the PIC grid requirement in which the grid size is smaller than several times of Debye length, and is surrounded by a dielectric of 0.2-cm thickness. The plasma region length L is set to 2.0 cm. Two pairs of the deflection antennae have 1.6-cm length and are centered in each edge. Applied AC voltage is a function of $V_0 \cos\omega t$ for the top and bottom antennae and $V_0 \sin\omega t$ for the left and right antennae, where $\omega = 2\pi f$. The magnetic field has the axial-direction component B_z and is assumed to be uniform and constant. To express the diverging magnetic field, we set the radial-direction magnetic field to $B_r(r) = B_{r0}\times r$, where B_{r0} has a positive value. The charged particles are considered for Ar^+ and e^-, and the initial temperatures are 0.5 eV and 5 eV, respectively. The initial plasma number density n_{p0} is uniformly set in the range of 10^{10}–10^{11} cm^{-3}. In this condition, the Debye length $\lambda_{De} \leq 5.3\times10^{-3}$cm; thus, the grid size is set to 5.0×10^{-3} cm and 480×480 grids are used. If the charged particles Ar^+ and e^- reach a dielectric, we let them be accumulated on the dielectric surface and the particle velocity is reset to 0 for describing loss of particle momenta.

With changing the parameters of V_0, f, B_z, B_{r0} and n_{p0}, we investigate a condition to achieve large azimuthal current J_θ and thrust.

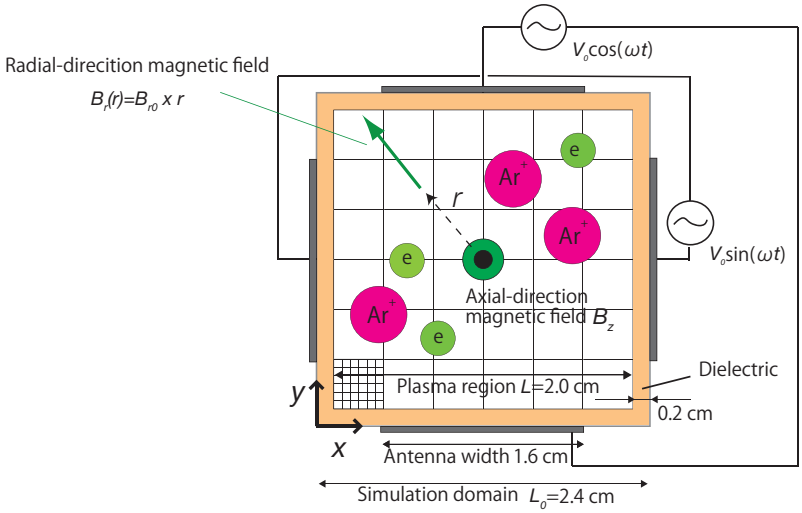

Figure 2. Simulation Conditions.

IV. Results and Discussions

A. Azimuthal current generation

Our past study shows that the condition producing large J_θ requires the ratio of the electron drift radius to the plasma region length R_D/L of ~0.3, high f, and $\omega_{ce} \gg \omega$ when the applied electric field fully penetrates.[7] As n_{p0} increasing, the electric field hardly penetrates into the plasma region because the plasma shielding effect becomes strong. However, applying high B_z and f improves the electric field penetration and produces large J_θ. For example, Fig. 3 shows the dependence of $\langle J_\theta \rangle$, which is averaged over the whole plasma region in 10 AC cycles, on B_z with $n_{p0} = 10^{10}$ cm^{-3} and $R_D/L = 0.28$. Note that no radial component of magnetic field is imposed in this section for simplicity. Since the high B_z suppresses the charge separation and the high f produces the higher rotating speed exceeding the field response against the charge separation, the electric field penetration is improved.

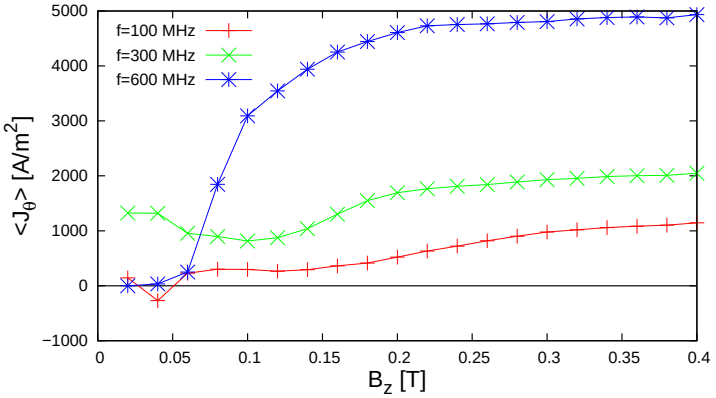

Figure 3. Dependence of $\langle J_\theta \rangle$ on B_z ($n_{p0} = 10^{10}$ cm^{-3}, $R_D/L = 0.28$).

We analyse the relation between J_θ and the electric field penetration based on a theoretical formula of the electric field penetration including the two-dimensional plasma rotating motion. The theoretical formula of electric field penetration are given by

$$\frac{E_{pg0}}{2V_0/L_0} = \frac{2}{\varsigma}(\sqrt{1+\varsigma} - 1), \tag{4}$$

$$\varsigma = \frac{8e\omega_{pe}^2}{m_e\omega^2\omega_{ce}^2 L_0}\frac{2V_o}{L_0}, \tag{5}$$

where $E_{pg0}/(2V_0/L_0)$ denotes a level with respect to the ideal strength.[6] Figure 4 depicts contours of $\langle J_\theta \rangle$ in a $B_z - f$ plane with $n_{p0} = 10^{11}$ cm^{-3} and $R_D/L = 0.28$. In the bottom-left corner region, $\langle J_\theta \rangle$ becomes negative because the electric field penetration is not sufficient. On the other hand, in the up-right region, $\langle J_\theta \rangle$ takes a large positive value since the electric field does not diminish and high f produces high rotating drift speed. Red and blue lines represent $E_{pg0}/(2V_0/L_0) = 0.5$ and 0.6, respectively, while yellow line denotes $\omega_{pe} = \omega_{ce}$ in Fig. 4. For $E_{pg0}/(2V_0/L_0) > 0.6$, $\langle J_\theta \rangle$ has a positive value. When $E_{pg0}/(2V_0/L_0)$~0.5, $\langle J_\theta \rangle$ becomes the lowest value (Fig. 4(b) clearly shows this tendency), because the charge separation with rotating plasma and plasma frequency are balanced. Moreover, in the area of $\omega_{pe} > \omega_{ce}$, the electric field hardly penetrates into plasma center region and the electric field is stronger in the outer region, because the effect that the magnetic field suppresses the charge separation is little or nothing. Thus, the rotating motion is only found in the outer region with high electric field, and $\langle J_\theta \rangle$ has a small positive value. Furthermore, this phenomenon also appears when $E_{pg0}/(2V_0/L_0)$ is relatively small value (the white color region for $B_z \geq 0.1$ T and $f \leq 200$ MHz in Fig. 4(b)). In these circumstances, we should choose the parameter of $E_{pg0}/(2V_0/L_0) > 0.6$ to produce J_θ leading to high acceleration.

The parameters of the past experiments were $n_{p0} = 10^{11} - 10^{12}$ cm^{-3}, $f \lesssim 100$ MHz, and $B_z \lesssim 0.1$ T corresponding to the left bottom in Fig. 4.[5] So, the electric field penetration is little or nothing, and the Lissajous acceleration is difficult to be found. To generate the Lissajous acceleration, higher B_z and f should be applied or n_{p0} is to be reduced.

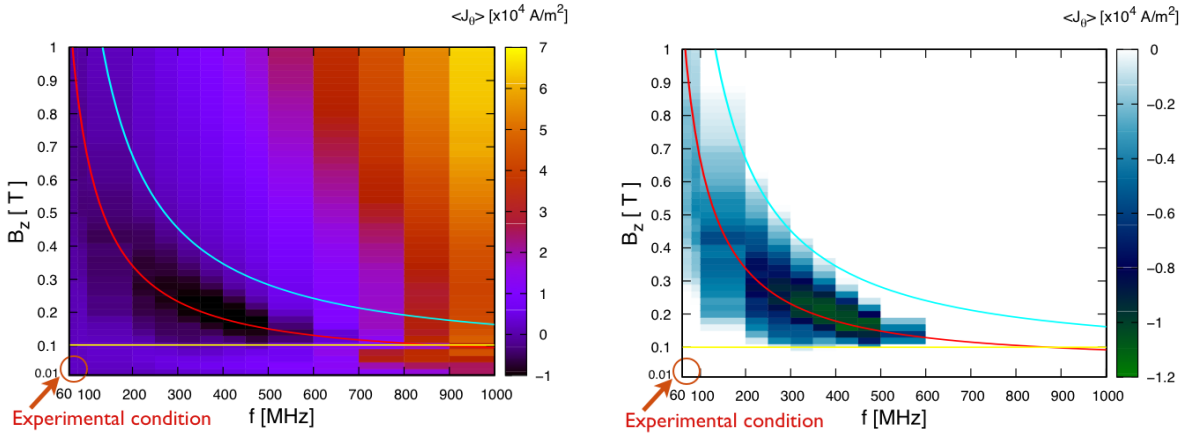

(a) Contours of $-1 \leq \langle J_\theta \rangle \leq 7$ [$\times 10^4$A/m^2]

(b) Contours of $-1.2 \leq \langle J_\theta \rangle \leq 0$ [$\times 10^4$A/m^2]

Figure 4. Contours of $\langle J_\theta \rangle$ in f–B_z plane (n_{p0} = 10^{11} cm^{-3}, R_D/L = 0.28).

B. Thrust estimation under radial magnetic field

In the previous section, J_θ tendency obtained by the simulations without B_r is presented. We next include B_r into the PIC simulations to estimate the Lissajous acceleration more directly.

Figure 5 shows contours of thrust F in a $B_z - f$ plane with $n_{p0} = 10^{11}$ cm^{-3}, $R_D/L = 0.28$, and $B_{r0} = 2.0\times10^{-3}$ T. The F is calculated after 5 AC cycles by

$$F = \sum_i |m_i n_i v_{zi}| v_{zi}. \tag{6}$$

After a few AC cycles, F becomes almost constant because the Lorentz force by $v_z \times B_r$ holds the Lissajous acceleration. The lines in Fig. 5 are the same lines in Fig. 4. In the area of $E_{pg0}/(2V_0/L_0) > 0.6$, F is a positive value, while for $E_{pg0}/(2V_0/L_0) \sim 0.5$, it becomes negative. Moreover, in the area of $\omega_{pe} > \omega_{ce}$, F shows a small positive value. Thus, the tendency of F is quite similar to the tendency of $\langle J_\theta \rangle$ obtained by the simulations without B_r. So, two-dimensional simulations without B_r may give us enough information to obtain the suitable parameters of the Lissajous acceleration.

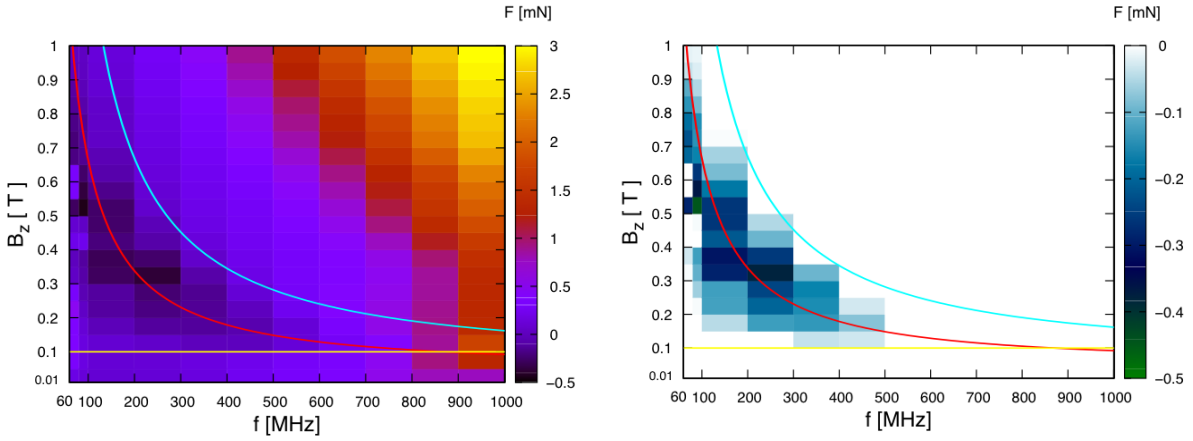

(a) Contours of $-0.5 \leq F \leq 3$ [mN]

(b) Contours of $-0.5 \leq F \leq 0$ [mN]

Figure 5. Contours of F in f–B_z plane (n_{p0} = 10^{11} cm^{-3}, R_D/L = 0.28, B_z = 0.5 T).

In order to examine an effect of B_r, additional simulations were carried out with different B_{r0}'s. Figure 6 shows the dependence of F on B_{r0} with $n_{p0} = 10^{11}$ cm^{-3}, $R_D/L = 0.28$, and $B_z = 0.5$ T. These conditions in Fig. 6 produce the positive value of $\langle J_\theta \rangle$ by the simulations without B_r. F is proportional to B_{r0} because the axial Lorentz force increases as B_{r0} increasing. However, too large B_{r0} results in loss of plasma momenta and then reducing F, since many plasma particles move along magnetic field line and reach to the dielectric. Therefore, F has a peak value in the parameter space. The peak value changes with the f value. With f = 700 and 800 MHz, the peak value is located at $B_{r0} \sim 0.01$

T. On the other hand, with f = 500 and 600 MHz, the peak point move to B_{r0}~0.015 T. In these cases, the electric field penetration is not ideal; therefore, higher B_r also improves the electric field penetration. We can conclude that the diverging magnetic field of B_{r0}/B_z~2% – 3% is suitable for the Lissajous acceleration.

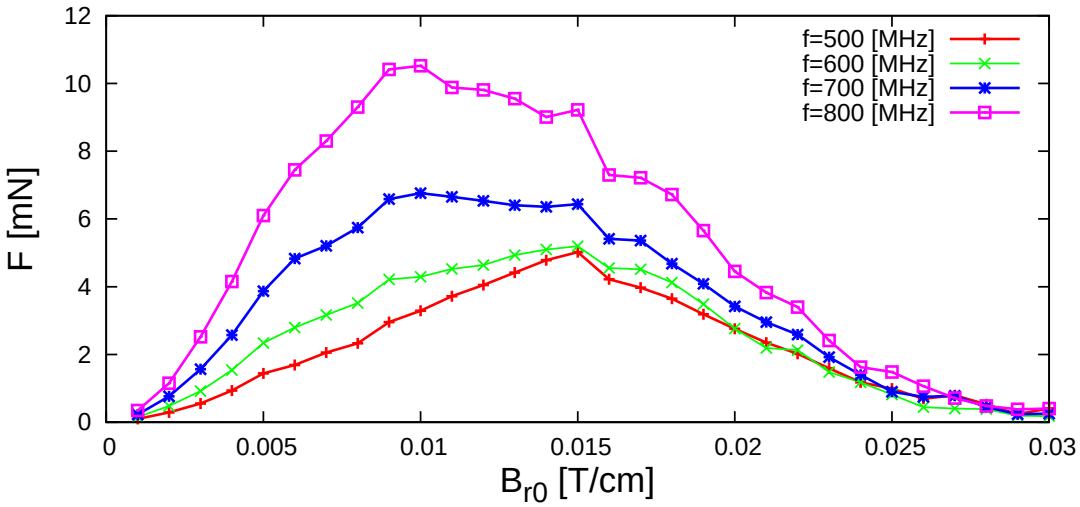

Figure 6. Relation between B_{r0} and F (n_{p0} = 10^{11} cm^{-3}, R_D/L = 0.28, B_z = 0.5 T).

To achieve larger F, we should choose a condition that large $\langle J_\theta \rangle$ and large B_{r0} as found in the simulation results. Higher B_z is also needed since the peak value is located B_{r0}/B_z~2% – 3%. Figure 7 shows the relation between B_{r0} and F with n_{p0} = 10^{11} cm^{-3}, R_D/L = 0.28, and B_z = 1.0 T. F reaches 10-mN order, and this is a level of the conventional Hall thruster.[11] If high B_z and f are applied, the electrodless plasma thruster with rotating electric field is promising as a next-generation thruster. However, the conditions that $B_z \geq$1.0 T and $f \geq$1000 MHz are not realistic in the present technology. So, we need further research to obtain the practical parameters for a real plasma thruster and space explorer.

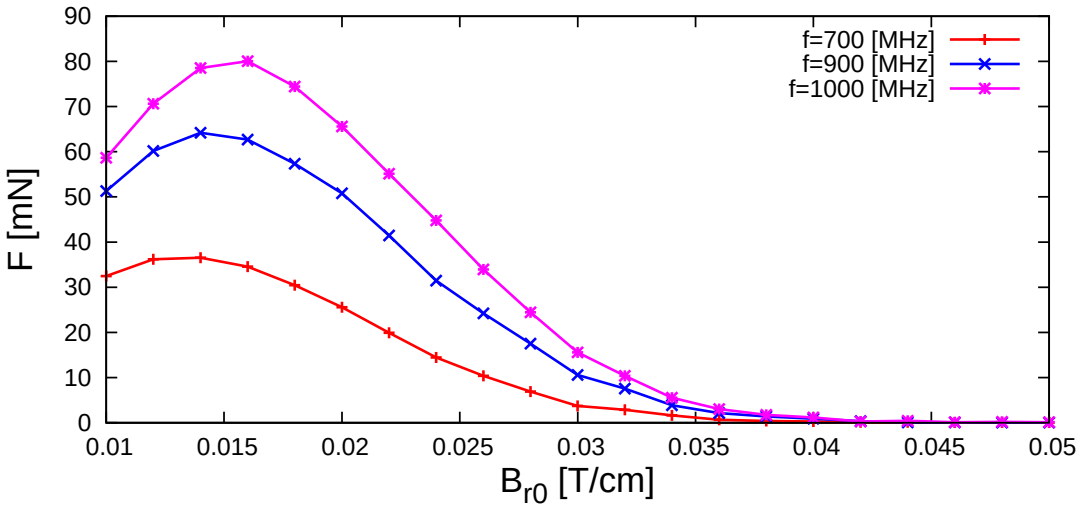

Figure 7. Relation between B_{r0} and F (n_{p0} = 10^{11} cm^{-3}, R_D/L = 0.28, B_z = 1.0 T).

V. Conclusions

Two-dimensional PIC simulations were conducted to research the optimal parameter to obtain large azimuthal current, Lissajous acceleration, and thrust in a cross section of the acceleration area of the electrodeless plasma thruster with rotating electric field and diverging magnetic field. The simulations without B_r shows that applying high B_z and f, the electric field penetration is improved and J_θ becomes a high positive value. When the electric field penetrates in a level of 0.6 with respect to the ideal strength, we can obtain a positive value of J_θ. The simulations with B_r shows that the condition corresponding to the large positive $\langle J_\theta \rangle$ in the simulations without B_r produces the large positive thrust. Moreover, the thrust has a peak value at $B_{r0}/B_z \sim 2\% - 3\%$. If we can use $B_z \geq 1.0$ T and $f \geq 1000$ MHz, several 10 mN is possible to be achieved, while such a condition is not practical at present.

In order to obtain an indication of the Lissajous acceleration in experiments, we must find the practical condition through more elaborate numerical simulations. Inductive electromagnetic field should be addressed for examining a practical condition of helicon plasma. Also, three-dimensional simulations may show the feasibility of the electrodeless plasma thruster in more realistic geometry.

References

[1]http://www.jaxa.jp/projects/sat/muses_c/index_e.html.

[2]H. Kuninaka, K. Nishiyama, I. Funaki, Y. Shimizu, T. Yamada and J. Kawaguchi, "Assesment of Plasma Interactions and Flight Status of the HAYABUSA Asteroid Explorer Propelled by Microwave Discharge Ion Engines", *IEEE Trans. Plasma Sci.*, vol. 34, 2006, pp. 2125–2132.

[3]S. Shinohara, T. Motomura, K. Tanaka, T. Tanikawa, and K. P. Shamrai, "Large-Area High-Density Helicon Plasma Sources", *Plasma Sources Sci. Technol.*, vol. 19, 2010, 034018.

[4]K. Toki, S. Shinohara, T. Tanikawa, I. Funaki and K. P. Shamrai, "Preliminary Investigation of Helicon Plasma Source for Electric Propulsion Applications", *Proc. of the 28nd IEPC*, IEPC-03-0168, 2003.

[5]T. Nakamura, K. Yokoi, H. Nishida, S. Shinohara, I. Funaki, T. Matsuoka, T. Tanikawa, T. Hada, K. P. Shamrai, and T. S. Rudenko, "Experimental Investigation of Plasma Acceleration by Rotating Electric Field for Electrodeless Plasma Thruster", *Proc. of the 32nd IEPC*, IEPC-2011-279, 2011.

[6]T. Matsuoka, I. Funaki, T. S. Rudenko, K. P. Shamrai, S. Satoh, T. Fujino, T. Nakamura, K. Yokoi, H. Nishida, S. Shinohara, T. Hada, and T. Tanikawa, "Progress in Development for Helicon Plasma Thrusters by Use of Rotating Electric Field (Lissajous Acceleration", *Proc. of the 32nd IEPC*, IEPC-2011-079, 2011.

[7]R. Nomura, N. Ohnishi and H. Nishida, "PIC Simulation of Electrodeless Plasma Thruster with Rotating Electric Field", *Proc. of 28th RGD, AIP Conf.*, vol. 1501, 2012, pp. 1431–1436.

[8]C. K. Birdsall and A. B. Langdon, *Plasma Physics via Computer Simulation*, Institute of Physics Publishing, London, 2004.

[9]H. Nishida, T. Nakamura, S. Shinohara, T. Matsuoka, I. Funaki, T. Tanikawa, T. Hada, and K. P. Shamrai, "Study on Proof-of-Principle of Lissajous Acceleration for Electrodeless Helicon Plasma Thruster", *Frontier of Appl. Plasma Technol.*, vol. 5, 2012, pp. 67–72.

[10]T. Matsuoka, T. S. Rudenco, I. Funaki, K. P. Shamrai, T. Nakamura, H. Nishida, T. Tanikawa, and S. Shinohara, "One Dimensional Modeling of Radio Frequency Electric Field Penetration into Magnetized Plasmas", *Jpn. J. Appl. Phys.*, vol. 51, 2012, 096201.

[11]D. Dignai, C. Ducci, G. Cifali, P. Rossetti, and M. Andrenucci, "HT-100 Hall Thruster characterization test results", *Proc. of the 32nd IEPC*, IEPC-2011-191, 2011.